Received: 9 December 2021 | Revised: 15 June 2022 | Accepted: 27 June 2022

DOI: 10.1002/jmor.21497

RESEARCH ARTICLE

JOURNAL OF morphology WILEY

The mouthparts of the adult dragonfly *Anax imperator* (Insecta: Odonata), functional morphology and feeding kinematics

Benedikt Josten | **Stanislav N. Gorb** | **Sebastian Büsse**

Department of Functional Morphology and Biomechanics, Kiel University, Kiel, Germany

Correspondence
Sebastian Büsse, Department of Functional Morphology and Biomechanics, Institute of Zoology, Kiel University, Am Botanischen Garten 9, 24118 Kiel, Germany.
Email: sbuesse@zoologie.uni-kiel.de

Funding information
Deutsche Forschungsgemeinschaft, Grant/Award Number: BU3169/2

Abstract

Insects evolved differently specialized mouthparts. We study the mouthparts of adult *Anax imperator*, one of the largest odonates found in Central Europe. Like all adult dragonflies, *A. imperator* possesses carnivorous-type of biting-chewing mouthparts. To gain insights into the feeding process, behavior and kinematics, living specimens were filmed during feeding using synchronized high-speed videography. Additionally, the maximum angles of movement were measured using a measuring microscope and combined with data from micro-computed tomography. The resulting visualizations of the 3D-geometry of each mouthpart were used to study their anatomy and complement the existing descriptive knowledge of muscles in *A. imperator* to date. Furthermore, confocal laser scanning microscopy-projections allow for estimation of differences in the material composition of the mouthparts' cuticle. By combining all methods, we analyze possible functions and underlying biomechanics of each mouthpart. We also analyzed the concerted movements of the mouthparts; unique behavior of the mouthparts during feeding is active participation by the labrum and distinct movement by the maxillary laciniae. We aim to elucidate the complex movements of the mouthparts and their functioning by combining detailed information on (1) in vivo movement behavior (supplemented with physiological angle approximations), (2) movement ability provided by morphology (morphological movement angles), (3) 3D-anatomy, and (4) cuticle composition estimates.

KEYWORDS

cuticle, dragonflies (Anisoptera), feeding, insects, material composition, morphological movement angles

1 | INTRODUCTION

Insects display a wide variety of mouthpart adaptations (Krenn, 2019; Snodgrass, 1935). While they are generally classified by their respective method of food uptake, their functions extent beyond feeding. Functions include, but are not limited to: predation, defense, combat, pest control, parasitization, recycling of nutrients, boring holes for egg deposition, building shelters and carrying offspring (Krenn, 2019; Losey & Vaughan, 2006; Mauss, 2007; Moon et al., 2008; Scudder, 2009; Snodgrass, 1935; Zhang et al., 2019). With

functions like these, the ecological and economic aspects of the insect's environment are affected considerably (Krenn, 2019; Weisser & Siemann, 2008). Examining form, function and kinematics of insect mouthparts may help understanding the correlation between functional morphology and ecological influence.

Dragonflies are regarded as key predators within their habitat, implying a considerable ecological impact (Corbet, 2004). They are often observed performing daring flight maneuvers to catch their prey (Engel et al., 2013; Pfau, 1986; Rüppell & Hilfert, 1993) and all adult odonates share the same type of feeding apparatus: biting-chewing mouthparts (Crampton, 1923; Matsuda, 1965; Tillyard, 1917). The blue emperor dragonfly is one of the largest species of dragonflies and one of the largest insects found in Central Europe. Due to their size, the mandibles of these dragonflies can generate considerable bite forces (David et al., 2016). The adult head anatomy of odonates, including the mouthparts, has previously been covered by numerous publications (Asahina, 1954; Blanke et al., 2012; Blanke et al., 2015; Pritchard, 1965; Tillyard, 1917); however, the kinematics of the mouthparts during feeding have rarely been studied in adult dragonflies (David et al., 2016). Popham and Bevans (1979) provided an elaborate overview of the feeding process on the example of larval and adult *Aeshna juncea* (Odonata: Anisoptera: Aeshnidae); insights into the larval feeding were given by Büsse et al. (2021a) and into the prey capturing process by Büsse et al. (2021b). Here, we expand on these studies with the example of *Anax imperator* Leach, 1815, or blue emperor dragonfly (Odonata: Anisoptera: Aeshnidae). In general, studies on the insect feeding process/kinematics, especially in combination with 3D-anatomy, are scarce and often focus on mandibles only (David et al., 2016; Weihmann et al., 2015). One example, covering all mouthparts, is the work of Schmitt et al. (2014) on *Periplaneta americana* (Blattodea: Blattidae), describing movement patterns of the mouthparts using X-ray cinematography. Furthermore, Hao et al. (2020) carried out an extensive study on the functional morphology of the mouthparts of the lady beetle *Coccinella transversoguttata* (Coleoptera: Coccinellidae). They focused on identifying different types of sensilla found on the mouthparts, subsequently drawing conclusions regarding their specific function.

The material composition of the insect cuticle becomes increasingly important for functional morphology and bio-mechanical research due to its complex composite and often graded structure (Andersen, 1979; Vincent & Wegst, 2004). Especially resilin, a viscoelastic, extracellular protein-matrix (Lerch et al., 2020; Weis-Fogh, 1960; Weis-Fogh, 1961), plays an essential role in a multitude of functions such as: (i) reducing wear and the risk of structural failure (e.g., Bäumler & Büsse, 2019; Haas et al., 2000a, 2000b), (ii) improving fatigue resistance (e.g., Haas et al., 2000a, 2000b; Rajabi et al., 2016a), (iii) allowing energy storage for high-speed movements (e.g., Burrows & Sutton, 2012; Büsse et al., 2021b; Gorb, 2004) or in insect attachment devices (e.g., Büscher et al., 2021; Büsse et al., 2019; Jandausch et al., 2018; Peisker et al., 2013; Petersen et al., 2018). The cuticular material composition of damselfly (Büsse & Gorb, 2018) and dragonfly (Büsse et al., 2021a) larval mouthparts has recently been studied. Comparable data on the mouthparts of adult Odonata has not yet been published.

A combination of the morphological data for all mouthparts linked with the kinematics of the feeding process is missing for adult odonates, making them a promising starting point to establish a workflow for broadscale comparison. To approach this, we combined micro-computed tomography (μCT), confocal laser scanning microscopy (CLSM), synchronized high-speed videography and measuring microscopy, to study the functional morphology of mouthparts and feeding kinematics in *A. imperator*. Using μCT, the mouthparts and the associated muscles were examined and detailed information about 3D-geometry of the mouthparts and muscle attachment sites was obtained. The head musculature of *A. imperator* was identified and listed by Blanke et al. (2013) and we expand on this knowledge by providing three-dimensional information. The importance of such analyses in the context of biomechanical studies has been shown by, e.g., Gröning et al. (2013), who performed a simulation of biting forces based on a lizard skull and showed that even small deviations in the data on the muscle fiber length alters the resulting bite force considerably.

Here, we address the following topics: (1) identify functionality or mobility by relating muscle insertions (μCT) to local cuticular material composition (CLSM); (2) observe said functions during in vivo feeding (HS-videography); (3) measure the morphologically possible movement (mma's) to identify the working zone of each mouthpart and combine the data with the 3D-geometry (μCT) of the respective mouthparts; (4) characterize behavioral traits during in vivo feeding (HS-videography). Insect mouthparts represent a highly distinctive model system, from ecology to bio-inspired robotics. The combination of methods presented in this study allows for an in-depth examination of the complex functional morphology of the mouthparts and feeding kinematics. This work aims to provide a base for future insect feeding physiology research and could be further refined to create possibilities of comparing other insects regarding their morphology and feeding behavior.

2 | MATERIALS AND METHODS

2.1 | Specimens

A total of 10 specimens of *A. imperator* Leach, 1815 were used for the analysis. Larvae were collected in Oeversee, Schleswig-Flensburg, Schleswig-Holstein, Germany in 2017, with permission of Helmut Jeske (landowner) and the State Government of Schleswig-Holstein (Landesamt für Landwirtschaft, Umwelt und ländliche Räume des Landes S.-H., Hamburger Chaussee 25, 24220 Flintbek, permission valid until August 2028). The larvae were reared in the lab using a set of water containers, at room temperature and with natural lighting conditions. The containers were equipped with sticks, giving the animals an opportunity to emerge. They were fed with *Chironomus plumosus* (Diptera: Chironomidae; Newman, 1834) larvae. The experiments were conducted after adult emergence (min. 72 h) and data recording was completed within approximately 2 weeks.

2.2 | Micro-computed tomography

For µCT, the specimens ($n = 2$) were CO_2 gas-flushed for anesthesia, dissected (removal of abdomen and legs), pre-fixed using Bouin's solution and stored in 70% ethanol. The samples were then dehydrated in an ethanol series and critically point dried (Balzers CPD030, Bal-Tec AG, Liechtenstein). The samples were scanned using a Skyscan 1172 µCT (Bruker micro-CT, Kontich, Belgium) with following settings: 180° scan; 40 kV; 250 µA; 0.25° rotation steps; voxel size: 4 µm. The resulted TIFF-images were reconstructed using the program Nrecon Ver. 1.7.5.9 (Bruker). The subsequent segmentation of the mouthparts was done using the program Amira Ver. 6.0.1 (Thermo Fisher Scientific). For further three-dimensional visualization and refining, the program Blender Ver. 2.8 (Blender Foundation, Amsterdam, Netherlands; General Public License) was used.

2.3 | Confocal laser scanning microscopy

The specimens ($n = 3$) used for CLSM were freshly frozen and stored (−70°C). Mandibles, maxillae, labrum and labium were dissected from the head. Each mouthpart was embedded in glycerin (99%). The scans were conducted using a Zeiss LSM 700 (Carl Zeiss Microscopy GmbH), with the wavelengths 405, 488, 555, and 639 nm and emission filters BP420–480, LP490, LP560, LP640 nm (cf. fig. 1 in Büsse & Gorb, 2018). The resulting data, mixed autofluorescence signals detected in each pixel, were combined into maximum intensity projections using the program ZEN 2008 (www.zeiss.de/mikroskopie).

CLSM, in this application method, allows determining regions of the insect cuticle containing certain components based on their corresponding autofluorescence. The observed material compositions can generally be subdivided into three main groups (after Michels & Gorb, 2012): (1) sclerotized cuticle showing red autofluorescence; (2) strong but relatively flexible, chitinous areas showing a range of colors from red over green to blue; (3) mostly flexible materials, like resilin-bearing cuticle, characterized by a violet or blue color.

Material composition estimates of the cuticle of *A. imperator* mouthparts have been visualized using CLSM as an indirect method of identifying occurrences of resilin-matrices in the insect cuticle by the di- and trityrosines interlinking pro-resilin monomers (Andersen, 1963, 1964); with different modifications of these matrices most likely leading to varying cuticle flexibility (Lerch et al., 2020). The CLSM-configuration detects the emissions specific to the bindings, and therefore, is regarded as an indirect method of locating resilin, as it does not necessarily give information about resilin-matrix-gradients. Further, it is highly likely that there are many more unknown proteins that could facilitate flexibility of the cuticle (Lerch et al., 2020). For the sake of brevity, we refer to the observed areas of blue autofluorescence as "resilin-supplemented," leaving room for interpretation on other components of the cuticle. While the results can be used as a qualitative approach to discuss the material composition, the effectivity of the method remains subject to debate. For example, the composition of the resilin-matrices can vary, thus influencing the mechanical properties (Lerch et al., 2020). The latter being dependent on fiber orientation and layer thickness of the cuticle (Vincent & Wegst, 2004), which is not recognized by CLSM. Also, the thickness of the endocuticle might influence the maximum intensity projections of the CLSM, possibly leading to misinterpretations of the resilin content of the exocuticle (Jansen et al., 2021). Thus, the CLSM-results herein are based on correlations found in studies combining the qualitative analysis of CLSM described originally in Michels and Gorb (2012) with quantitative measurements from atomic force microscopy (e.g., Peisker et al., 2013) or nano indentation (e.g., Li et al., 2021). In these studies, the material composition described by the CLSM autofluorescence correlates with the material properties from the indentation as described above—on particular body parts of some insects. However, even though CLSM is a solely qualitative method describing the material composition of the visualized cuticle, various studies underline its value for functional implications.

2.4 | Morphological movement angles (mma's)

The mma's were measured using five specimens ($n = 5$), the final result being the average out of those five measurements, for each separate direction of movement. The head capsules of the specimens were separated from the thorax and fixed on a Petri dish using dental wax (polyvinylsiloxane, President light body; Coltene), so that the mouthparts were facing up without contact to the dental wax or anything else. The dish with the specimen was placed on a Mitutoyo MF-U510TH measuring microscope (Mitutoyo, Kawasaki) (Supporting Information Online Material, Figure S1A) and all mouthparts were marked using white modeling color (Figure S1B, S2). The measurements were executed, beginning with the labium and ending with the labrum. The coordinates (x/y/z) of each point were determined, once in a resting position of the mouthpart and again, when the mouthpart was manually deflected to its maximum. It was fixed at this maximum position using insect pins, which were pierced into the wax inside the dish. The coordinates of each mark in resting position and at maximum deflection were used to calculate the angles between both positions using the dot product (Figure S3). To ensure the correct calculation, the marks on the mouthpart were assigned along a shared rotational axis with the joint or joint-like structure in case these were not directly visible. Due to the lack of a corresponding joint-like structure for the retracting movements of labrum and maxilla, we calculated the vector length between the resting and retracted position of the same point, which resulted in the distance traveled during retraction. The resulting angles and distances were used to define the working zone of the respective mouthpart and interpreted as estimations of the maximum opening angles and distances. For more information on mma measurements we refer to Gorb (1995, 2004) or Frantsevich et al. (1996).

2.5 | Behavior and physiological angle approximations (paa)

Living specimens (n = 4) were fixed to a custom-made specimen holder using dental wax. Two high-speed video cameras were synchronized to record the specimens, one from a frontal view and the second from a fronto-lateral view (Figure S4) with a framerate of 250 fps and a resolution of 1024 × 1056p. Both cameras were synchronized and filmed 11 s of footage once triggered. The setup was illuminated by two spotlights (AEOS 2, Rotolight). Examples of the resulting recordings can be found in supplementary online material, Videos S1–S4). To initiate the feeding process, houseflies were attached to a toothpick using dental wax (Figure S5) and fed to the dragonfly. A total of 182 separate feeding cycles have been identified from 40 recordings (10 for each specimen). Not all mouthparts were completely visible in every recorded feeding process due to being partially covered by food items, thus the number of approximated angles is lower especially for the labrum and the maxillae.

Determining approximations of the physiological angles (paa's) was more challenging than measuring the mma's. Many approaches for tracking of objects moving in a three-dimensional space can been applied (El-Gohary & McNames, 2012; Knoop et al., 2006; Mathis et al., 2018; Nath et al., 2019; Qian & Chen, 2017; Theriault et al., 2010). However, in almost all cases, the subject is moving freely, being observable and well-lit from all sides over the course of the recording. The intention of characterizing the movement of mouthparts on the living animal restricted us from using these kinds of methods, since the joints or joint-like structures could not be directly observed in the videos, contrary to many examples found in literature on vertebrates (e.g., El-Gohary & McNames, 2012; Knoop et al., 2006). Additionally, the bulky labium and especially the large labial palps obstructed the lateral view on other mouthparts like the maxillae, often casting shadows. These shadows complicated automated tracking and are unavoidable without damaging the labium. We, therefore, used a graphical approach to determine the opening angles, to avoid otherwise necessary manipulation of the mouthparts by measuring projected angles on the videos using the program Kinovea (Joan Charmant, Bordeaux, France, General Public License). For example, we measured the distance between the tip of the largest incisivus and the posterior mandibular condyle; we projected this distance on the head of *A. imperator* from the point of view of our camera (for reference see Figure S6A,B). The imposed angle would be positioned at the dorso-ventral center of the frons, making this point the reference for our angle vertex. In Kinovea, we then positioned the overlay on the first frame of the feeding cycle, when the mandible was still closed (Figure S6C). The first ray of the angle was placed on the tip of the incisivus in resting position, the second ray on the same tip when the mandible is deflected to the maximum of that specific feeding cycle (Figure S6D). This results in an approximation of an angle with similar parameters as the mma's, like the distance between measuring point and angle vertex. This procedure was repeated with all mouthparts and movement directions with similar joint-like structures. Exceptions from this are the retraction of the maxillae and labrum. Due to the lack of joint-like structures, we used the same reference points to approximate the distance traveled. For each identified movement cluster (opening and subsequent closing of the mouthparts), all paa's of the visible mouthparts were measured. This method, however, has limitations, which prevents us from using the measurements as quantitative data: (1) The amount of uncertainty while placing the overlay and measuring the angle is considerable, due to distance alterations caused by the perspectives and the movement of the dragonfly head itself; (2) By using a substitute point on the frons as an angle vertex, the resulting angle must be viewed as being inherently different from the mma, since the vertex of the paa is not placed on the rotational axis of the mouthpart. This can lead to further uncertainty by, for example, skewed perspective, therefore, the paa merely represents an approximation of an angle with similar parameters to the mma. These restrictions make the comparison of mma's and paa's difficult and the latter should only be regarded as qualitative supplemental results for the behavioral observations, not as quantitative measurements.

3 | RESULTS

3.1 | Mouthpart anatomy

Figures 1–4 show the 3D-visualizations of the head capsule, the mouthparts and their muscles in *A. imperator*. A complete list of all abbreviations used and all muscles found is provided in Supporting Information Online Material, Tables S1 and S2, respectively.

3.2 | Labrum

The labrum (lb, Figure 1) is roughly kidney-shaped from a frontal view and anterior-posteriorly flattened. It connects to the ventral edge of the anteclypeus (aclp) and is suspended to the head capsule via the clypeal suture. The labrum is slightly rounded, both lateral edges being curved towards the head capsule. The epipharynx is located on the abdominal side of the labrum.

3.2.1 | Musculature

M. frontolabralis (0lb1)—O: Interantennal ridge, mesal of 0lb2 at the mesal section of the ridge. I: Medial on the dorsal wall of the labrum. *M. frontoepipharyngalis* (0lb2)—O: Interantennal ridge, lateral of 0lb1. I: Dorsal lateral wall of the tormae. *M. labroepipharyngalis* (0lb5)—O: Inner anterior labral wall. I: broadly on the inner wall of the epipharynx. *M. epistoepipharyngealis* (0lb3), *M. labralis transversalis* (0lb4), *M. labrolabralis* (0lb6)—absent.

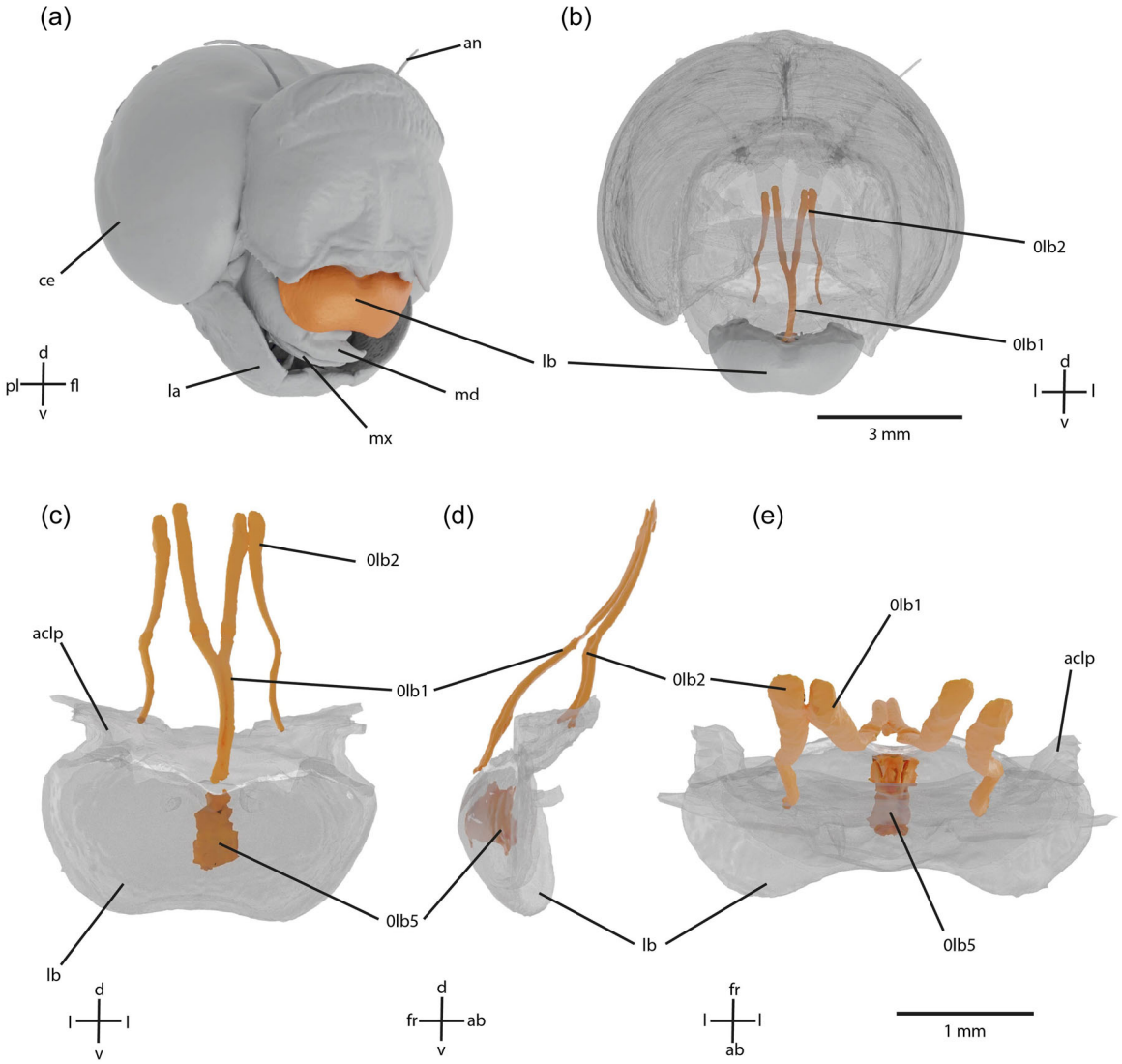

FIGURE 1 *Anax imperator*, three-dimensional visualization of the head, labrum and labral muscles based on micro-computed tomography data. (a), fronto-lateral view on the head capsule; (b), frontal view on the transparent head capsule; (c–e), labrum and labral muscles from frontal view (c), lateral view (d) and dorsal view (e). aclp, anteclypeus; an, antenna; ce, compound eye; la, labium; lb, labrum; md, mandible; mx, maxilla

3.3 | Mandibles

The mandibles (md, Figure 2) have a well-developed incisor area, consisting of multiple incisivi joining into a broad base. Other teeth form an articulated z-shaped molar lobe visible from a lateral view. The mandibles have posterior and anterior articulations for suspension. They are opened on the proximal side, thus allowing mandibular muscles to insert into the inner walls.

3.3.1 | Musculature

M. craniomandibularis internus (0md1)—O: Large areas of the posterolateral and posterodorsal head capsule. I: Adductor tendon in the dorsal edge of the mandible. *M. craniomandibularis externus posterior* (0md3)—O: Posterior area of the head capsule, ventral of 0md1. I: Abductor tendon in the posterior laterodorsal edge of the mandible. *M. hypopharyngomandibularis* (0md4)—O: Suspensorial bar of the hypopharynx. I: Posterior inner wall of the mandible. *M. tentoriomandibularis lateralis superior* (0md5)—O: Tentorium, on the distal part of the anterior arm. I: Posterior inner wall of the mandible, posterior to 0md4. *M. tentoriomandibularis lateralis inferior* (0md6)—O: Anterior tentorial arm. I: Anterior inner wall of the mandible, ventral of 0md4. *M. tentoriomandibularis medialis inferior* (0md8)—O: Anterior tentorial arm, sharing a tendon with 0md6. I: Posterior inner wall of the mandible. *M. craniomandibularis externus anterior* (0md2), *M. tentoriomandibularis medialis superior* (0md7)—absent.

3.4 | Maxillae

The maxillae (mx, Figure 3) can be subdivided into four parts: cardo (ca), stipes (st), maxillar palp (mpl) and lacinia (lac). The cardo is

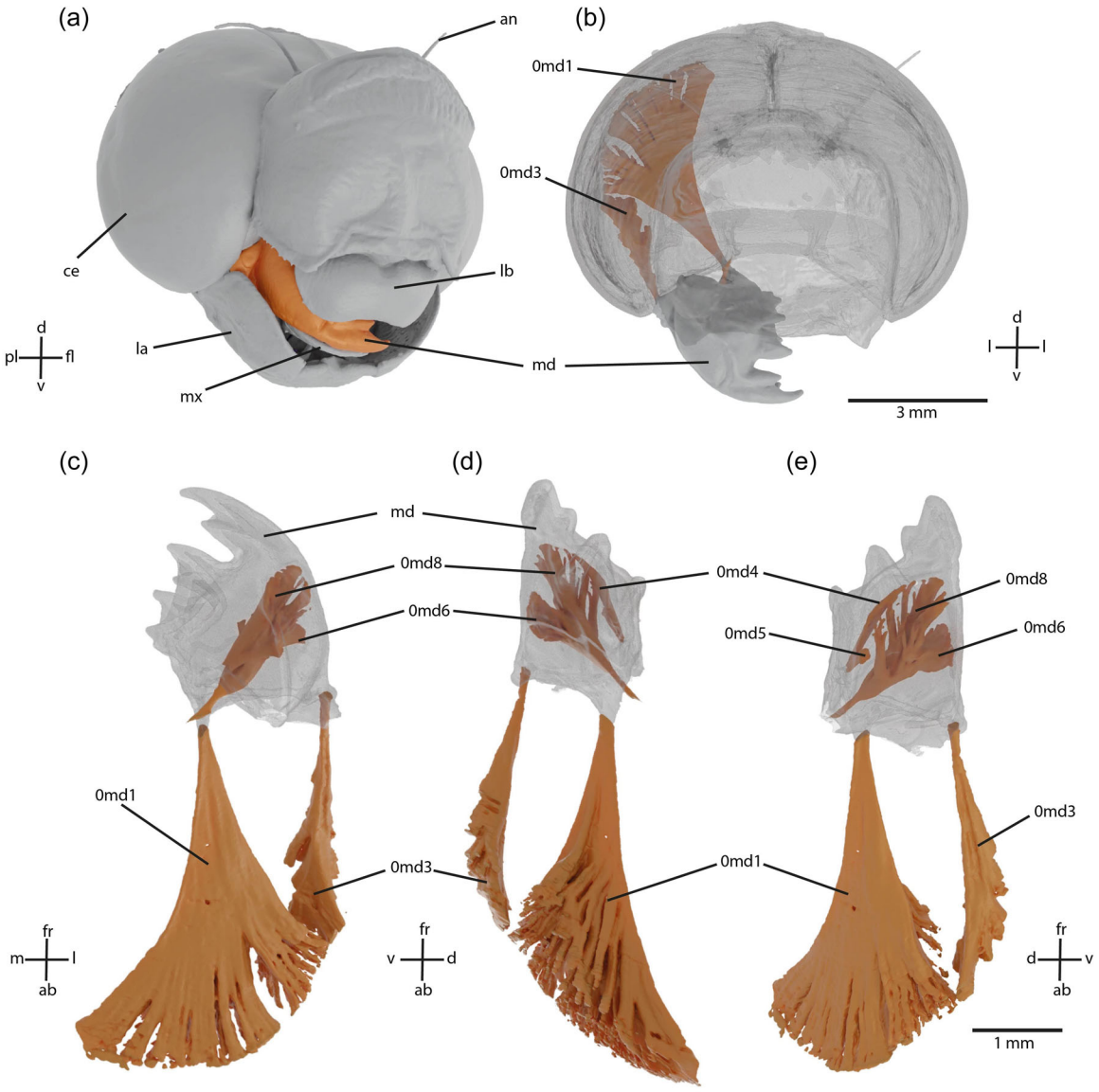

FIGURE 2 *Anax imperator*, three-dimensional visualization of the head, mandible and mandibular muscles based on micro-computed tomography data. (a) fronto-lateral view on the head capsule; (b) frontal view on the transparent head capsule; (c–e) mandible and mandibular muscles from dorsal view (c), median view (d) and lateral view (e). an, antenna; ce, compound eye; la, labium; lb, labrum; md, mandible; mx, maxilla

triangular, and the stipes is long and slender. Both the maxillar palp and the lacinia originate from the distal end of the stipes. The lacinia possesses two articulated maxillary incisivi as well as multiple dentisetae. The maxillae are suspended to the head capsule via the tentorial bridge inserting into the cardo and membranes connecting the stipes to parts of the head capsule.

3.4.1 | Musculature

M. craniocardinalis (0mx1)—O: Between 0md1 and 0md3 in the posterolateral part of the head capsule. I: base of the cardo. *M. craniolacinialis* (0mx2)—O: Posterolateral part of the head capsule, lateral to 0mx1. I: Base of the lacinia. *M. tentoriocardinalis* (0mx3)—O: Ventrolateral part of the anterior tentorial arm. I: Inner surface of the cardo. *M. tentoriostipitalis anterior* (0mx4)—O: Ventral side of the anterior tentorial arm. I: Ventral wall of the stipes. *M. tentoriostipitalis posterior* (0mx5)—O: Ventral base of the anterior tentorial arm, lateral to 0mx4. I: Posterior outer stipital wall. *M. stipitolacinialis* (0mx6)—O: Ventrolateral area of the stipital base. I: Base of the lacinia. *M. stipitopalpalis externus* (0mx8)—O: Lateral inner wall of the stipes. I: Posteriorly on the base of the palpus. *M. stipitopalpalis internus* (0mx10)—O: Lateral inner wall of the stipes. I: Anteriorly on the base of the stipes. *M. stipitogalealis* (0mx7), *M. stipitopalpalis medialis* (0mx9), *M. stipitalis transversalis* (0mx11), *M. palpopalpalis maxillae primus* (0mx12), *M. palpopalpalis maxillae secundus* (0mx13), *M. palpopalpalis maxillae tertius* (0mx14), *Musculus palpopalpalis maxillae quartus* (0mx15)—absent.

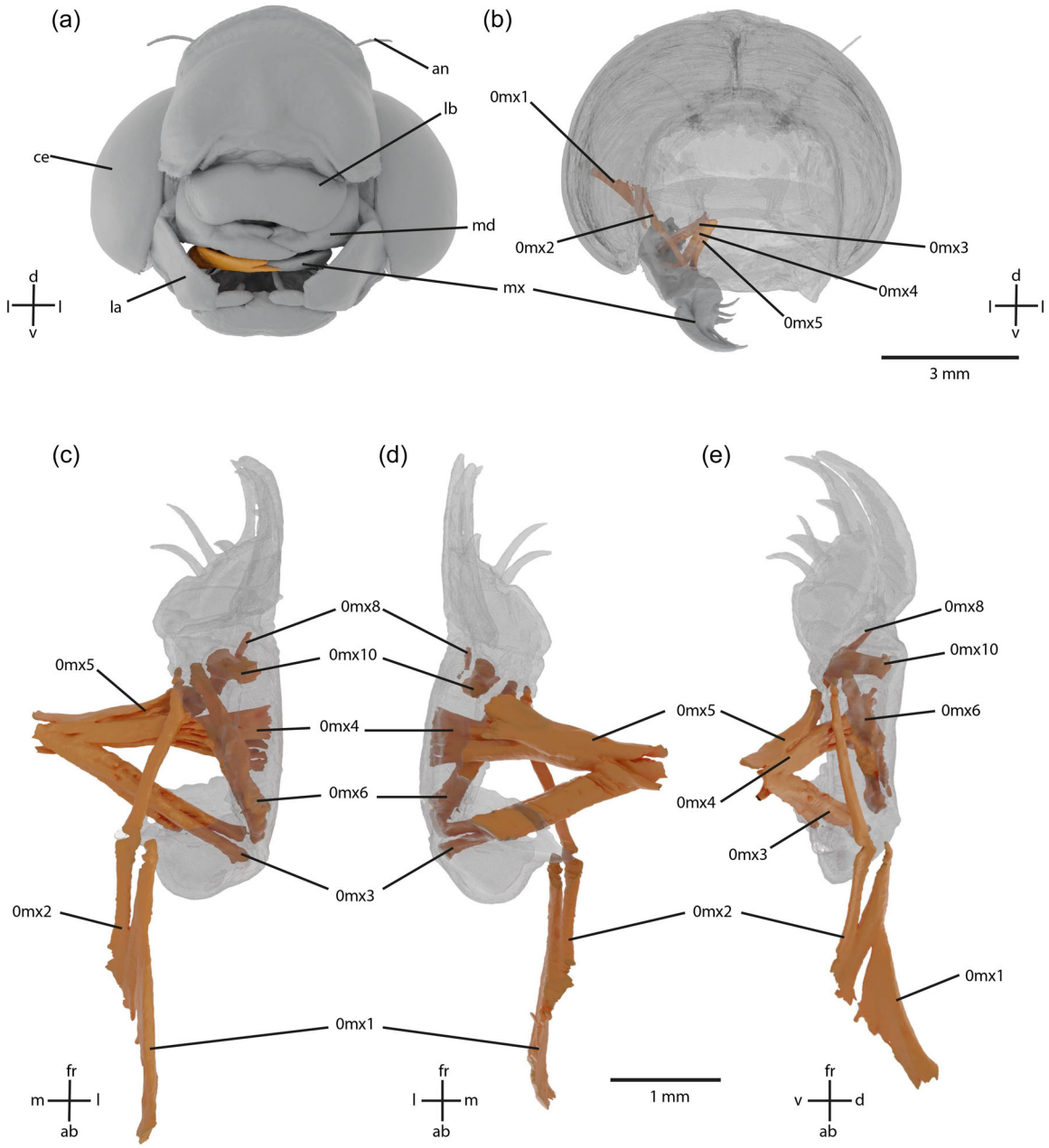

FIGURE 3 *Anax imperator*, three-dimensional visualization of the head, maxilla and maxillar muscles based on micro-computed tomography data. (a) frontal view on the head capsule; (b) frontal view on the transparent head capsule; (c–e) maxilla and maxillar muscles from dorsal view (c), ventral view (d) and median view (e). an, antenna; ca, cardo; ce, compound eye; la, labium; lac, lacinia; lb, labrum; md, mandible; mp, maxillar palpus; mx, maxilla; st, stipes

3.5 | Labium

The base of the labium (la, Figure 4) is separated into prementum (prm) and postmentum (pm). The postmentum is connected to the head capsule by a membranous area, the submentum. At the distal end of the prementum two labial palps (lp) as well as two large end hooks (eh) are developed. The labium is curved towards the other mouthparts and covers a large cavity of the mouth.

3.5.1 | Musculature

M. submentopraementalis (0la8)—O: Medially on the submentum. I: Base of the prementum. *M. praementopalpalis internus* (0la13)—O: Mesally on the prementum. I: Anterior base of the palpus. *M. praementomembranus* (0la15)—O: Mesally on the prementum. I: Dorsal membrane of the prementum. *M. postoccipitoglossalis medialis* (0la1), *M. postoccipitoglossalis lateralis* (0la2), *M. postoccipitoparaglossalis* (0la3), *M. postoccipitoprementalis* (0la4),

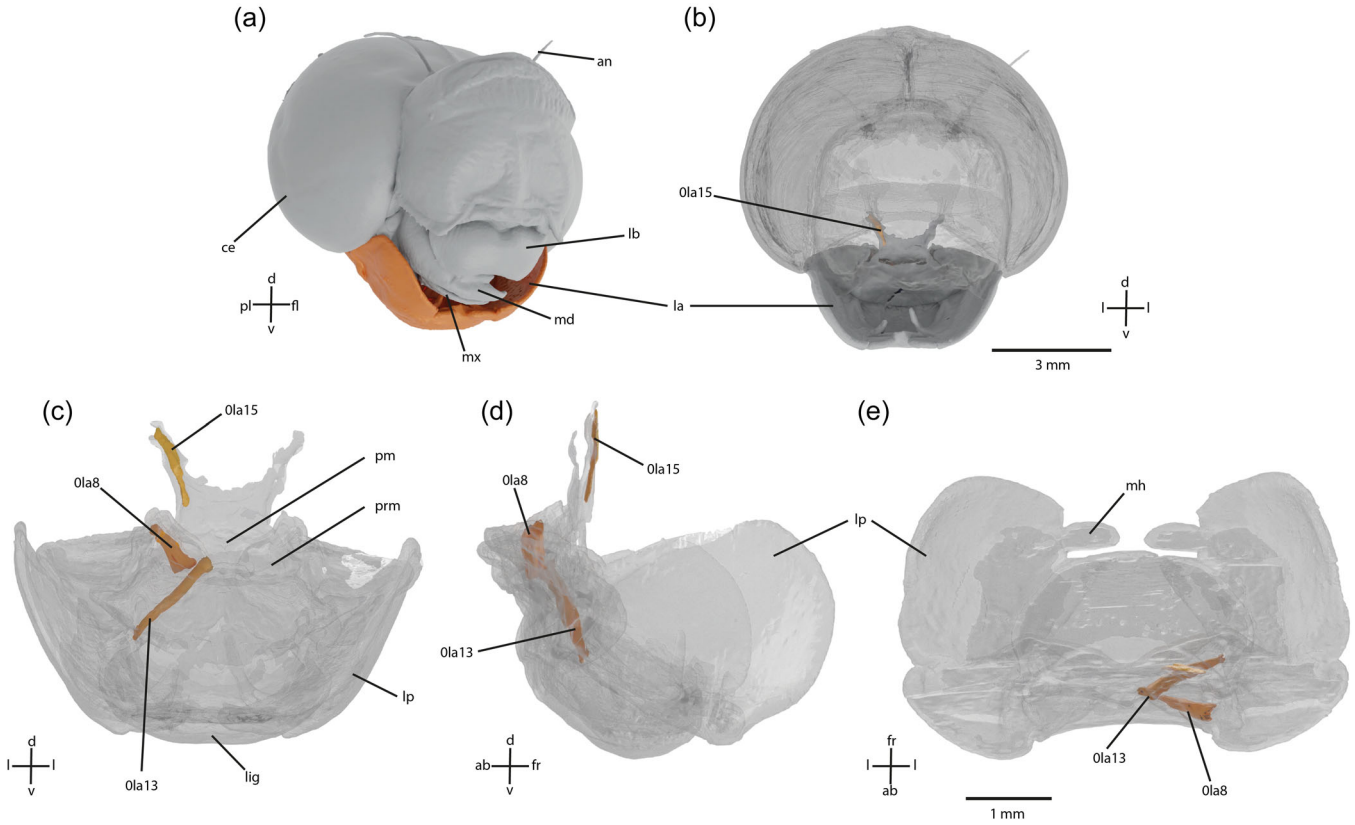

FIGURE 4 *Anax imperator*, three-dimensional visualization of the head, labium and labial muscles based on micro-computed tomography data. (a) fronto-lateral view on the head capsule; (b) frontal view on the transparent head capsule; (c–e), labium and labial muscles from frontal view (c), lateral view (d) and ventral view (e). an, antenna; ce, compound eye; eh, end hook; la, labium; lb, labrum; lig, ligula; lp, labial palpus; md, mandible; mh, movable hook; mx, maxilla

M. tentoriopraementalis (0la5), *M. tentorioparaglossalis* (0la6), *M. tentorioglandularis* (0la7), *M. postmentomembranus* (0la9), *M. submentomentalis* (0la10), *M. praementoparaglossalis* (0la11), *M. praementoglossalis* (0la12), *M. praementopalpalis externus* (0la14), *M. palpopalpalis labii primus* (0la16), *M. palpopalpalis labii secundus* (0la17)—absent.

4 | CLSM-IMAGING OF THE MOUTHPART CUTICLE

4.1 | Labrum

The frontal view of the labrum (Figure 5a) shows large dorsal areas of cuticle with blue autofluorescence. The clypeolabral suture (cls) is similar in emission. A clypeolabral bar (clb) and a clypeolabral pad (clp) are present. Numerous setae (set), covering the labrum ventrally, are green in the maximum intensity projection. A large ventral portion of the labrum is dark on the projection. On the abdominal side (Figure 5c), the epipharynx (ep) is covered with minute processes, some of which display a socket with red autofluorescence while others seem to be cuticular protrusions, also represented in red in the projection. The former occurs either singular or clustered. The abdominal side of the labrum is broadly covered by setae. There are also two large bundles of setae, joining at the base and facing towards the oral cavity. The cuticle of the epipharynx is mostly a mixture of blue and green in the projection. The base of the two large brushes (br; Figure 5c), however, is red, changing slightly towards green at the tips of the setae. The individual setae covering the surface of the labrum display green autofluorescence.

4.2 | Mandible

The incisive area (inc), as well as the molar lobe (ml), display red emissions (Figure 6). This is contrasted by a large area of blue autofluorescence on the aboral side of the mandible (the mandibular pad [mp]). The boundaries of this area show a relatively abrupt gradient into the surrounding cuticle of the mandible, which is a mixture of green and red. Setae are arranged in multiple distinctive lines, their positions being: along the lateral edge; abdominal of the molar lobe, ventral side; median above the anterior acetabular ridge (aar), ventral side; along the median molar ridge (mmr), describing a "L"-shape from the anterior mandibular articulation (pma) to the base of the incisivi. There are a few areas of the mandible, most notably at the base of the incisivi, which appear dark in the projection.

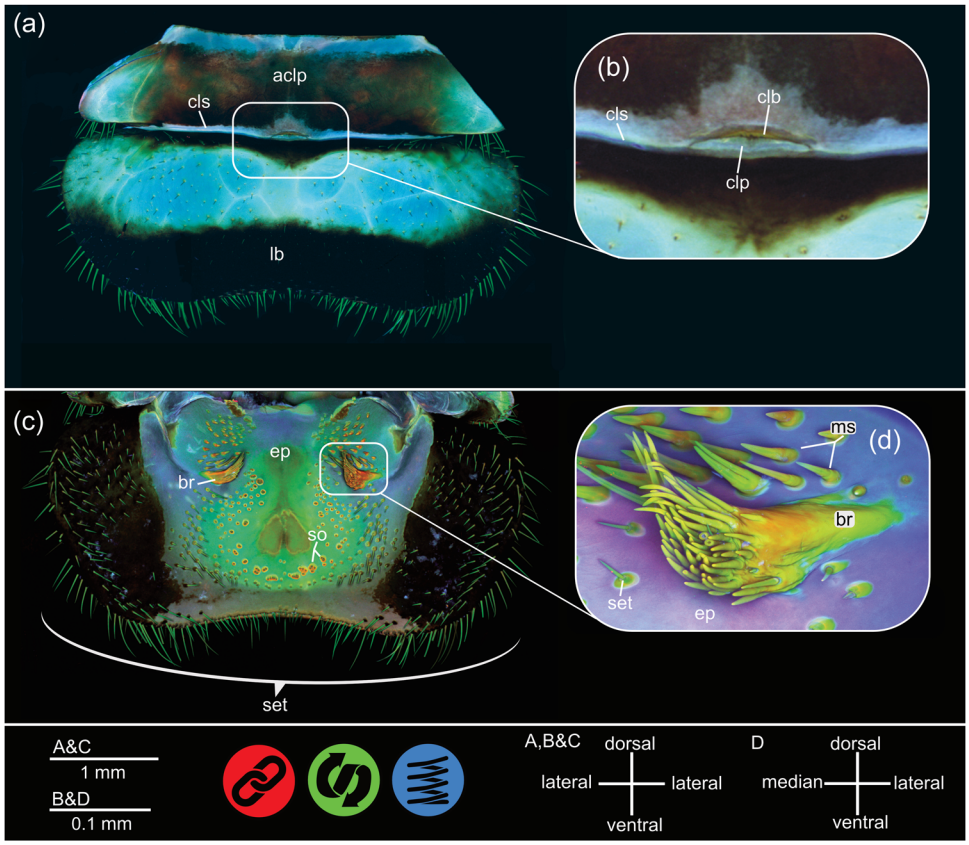

FIGURE 5 *Anax imperator*, maximum intensity projections of the labrum using confocal laser scanning microscopy data. (a) frontal view on the labrum; (b) frontal view on the clypeolabral bar and pad; (c) abdominal view; (d) large brush of setae. aclp, anteclypeus; br, brush of setae; clb, clypeolabral bar; clp, clypeolabral pad; cls, clypeolabral suture; ep, epipharynx; lb, labrum; ms, multicellular spines; set, setae; so, sensory organ

4.3 | Maxilla

The cardo (ca) of the maxilla emits blue autofluorescence on the projection. An exception is the suture (cardo-stipeal suture [css]) that connects the cardo to the stipes (st), which emits a mixture of blue and green (Figure 7a). The cuticle of the stipes displays a range from blue in the proximity of the cardo through green to a mixture of green and red autofluorescence towards the lacinia (lac). Furthermore, the stipital-lacinial suture (sls) displays blue emissions. The lacinia itself shows a mixture of green and red in the projections, while the base of the maxillar palpus (mpl) is blue. Both the dentisetae (dse) and the maxillar incisivi (inc) are red, possessing circular spots of blue autofluorescence at the base (Figure 7b), corresponding to the dentisetal pads (dsp).

4.4 | Labium

The labium, in frontal view, shows green emissions on a large part of the surface including the ligula (lig), with a slight tendency towards blue (Figure 8a). Exceptions to this are the labial hooks (movable hooks [mh]) which are red in the projection. The surface of the labial palps (lp) is covered by setae. In ventral view, the prementum (prm) shows blue autofluorescence (Figure 8b).

5 | MOVEMENT RANGE AND BEHAVIOR

In the 3D-visualizations (Figures 9–15) for each direction of movement, the transparent mouthpart models represent the relaxed state, while the opaque mouthparts represent the mouthpart in its adducted, abducted or retracted positions. The movement types are mirrored for both left and right mandibles and maxillae. Added to the models are the mma's (red), maximum paa's (dark blue) and median paa's (light blue). In the case of retraction of labrum and maxillae, the distance moved is displayed instead, with the same colors.

5.1 | Labrum

The movement of the labrum can be subdivided into the retraction into the head cavity until the labrum is almost out of sight (Figure 9a),

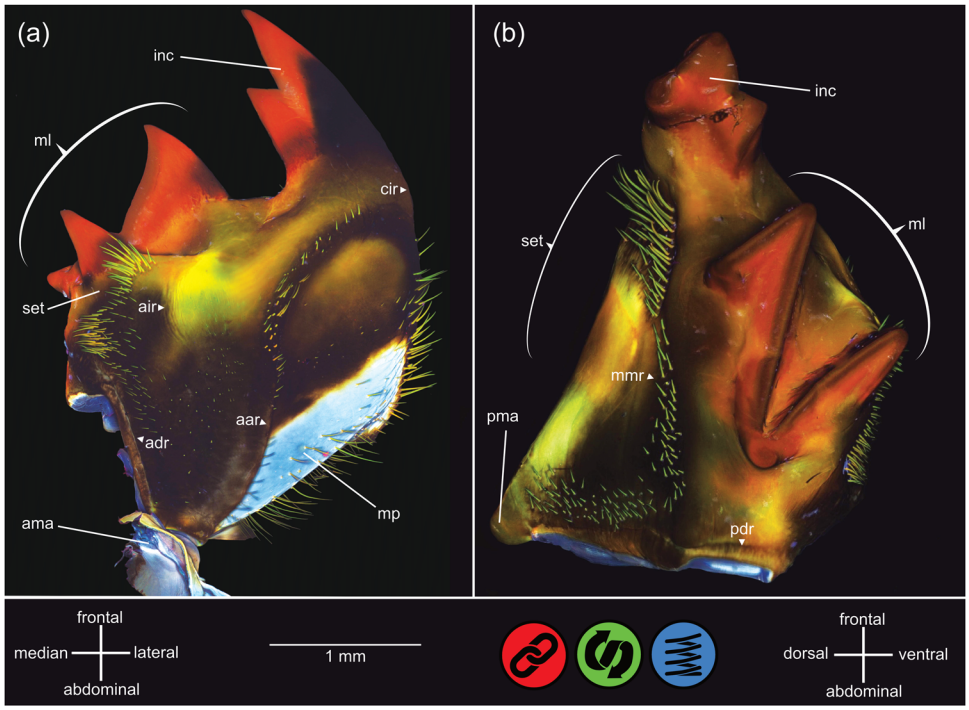

FIGURE 6 *Anax imperator*, maximum intensity projection of the mandible using confocal laser scanning microscopy data. (a) anterior view; (b) median view. aar, anterior acetabular ridge; ama, anterior mandibular articulation; adr, anterior dorsal ridge; air, acetabula—incisivi ridge; cir, condylar–incisivi ridge; inc, incisivus; ml, molar lobe; mmr, median molar ridge; mp, mandibular pad; pdr, posterior dorsal ridge; pma, posterior mandibular articulation; set, setae

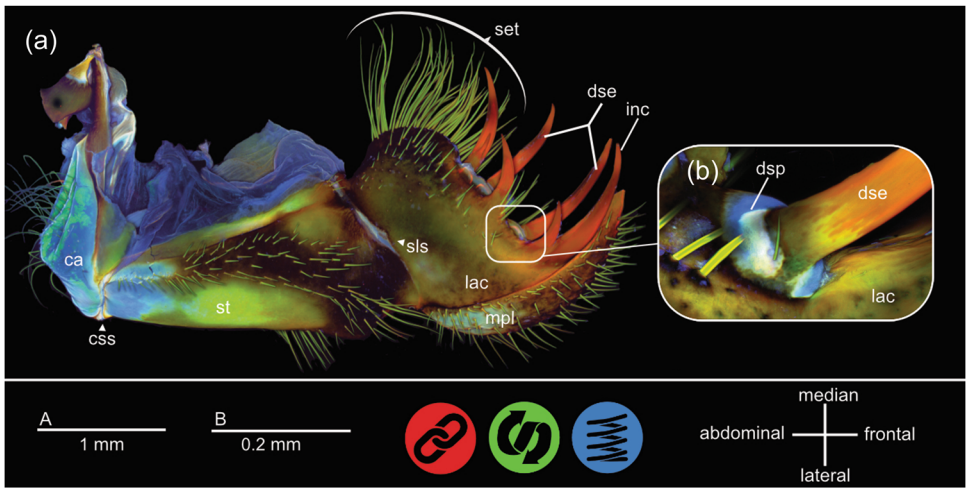

FIGURE 7 *Anax imperator*, maximum intensity projection of the maxilla using confocal laser scanning microscopy data. (a) Maxilla from dorsal view; (b) base of the dentisetae. ca, cardo; css, cardo-stipedial suture; dse, dentisetae; dsp, dentisetal pad; inc, incisivus (maxillar); lac, lacinia; mpl, maxillar palpus; set, setae; sls, stipito-lacinial suture; st, stipes

as well as an abducting motion towards the frontal direction (Figure 9b). While both motions were frequently observed during the feeding process, the labrum can also be moved into both lateral directions. This is a slight motion and was only occasionally observed during feeding. The median distance moved for the dorsal retraction is 1.29 mm and the mma measured for the abduction in frontal direction is 18.6°. It was also observed that the labrum is enlarged anterio-posteriorly during some feeding sequences.

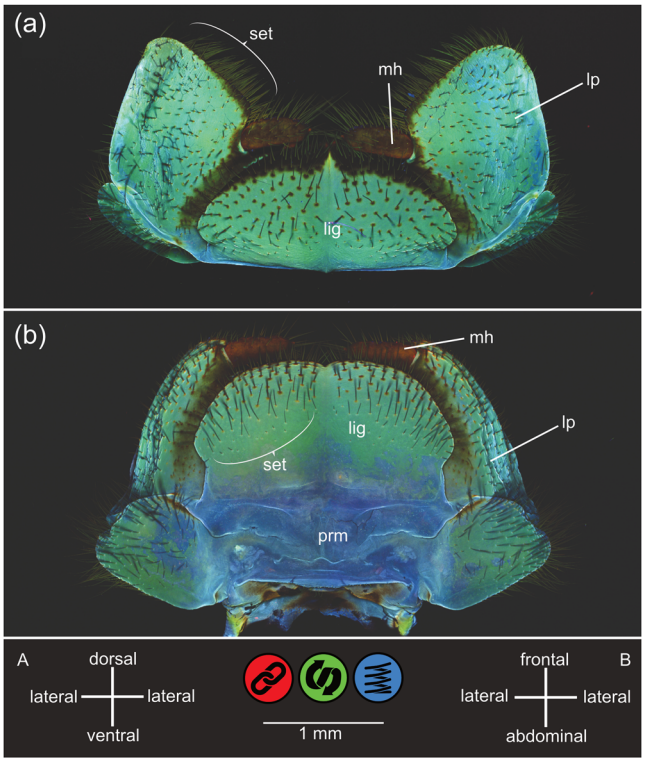

FIGURE 8 *Anax imperator*, maximum intensity projection of the labium using confocal laser scanning microscopy data. (a) Frontal view; (b) ventral view. lig, ligula; lp, labial palpus; mh, movable hook; prm, prementum; set, setae

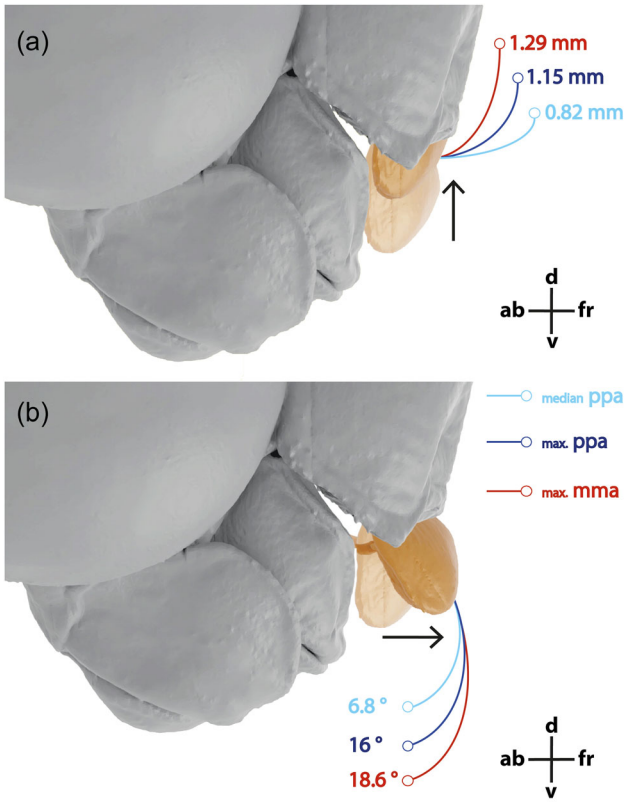

FIGURE 9 *Anax imperator*, visualization of the retraction (a, dorsal direction) and abduction (b, frontal direction) movements of the labrum, with maximum mma (red), maximum paa (dark blue) and median paa (light blue); lateral view.

5.2 | Mandibles

The movements of the mandibles are restricted by their two condyles to a single plane, i.e., an abducting and adducting motion (Figure 10). The mma's are 38.6° for the right mandible and 37.1° for the left mandible. In a few cases, it was observed that one mandible was opened wide, while the other one remained at almost initial position or only opened to a few degrees.

5.3 | Maxilla

The maxillae can be abducted (Figure 11), adducted (Figure 12) and they can be retracted towards the center of the head (Figure 13). Additionally, they can be tilted into a ventral direction (Figure 14). The mma for the lateral direction is 23.9° for the right maxilla and 24.3° for the left one. In median direction (adducting), the angles measured were 6.5° and 6.9°, respectively. When retracting, the distances were 0.71 mm for the right and 0.67 mm for the left maxilla. During abduction in the ventral direction, the angles were 18.9° for the right and 18.7° for the left maxilla. In some cases, the lacinia and palpus extended into view from behind the mandibles, before the entire maxilla is protracted (Video S1), indicating movement of both structures relative to the rest of the maxilla. We observed frequently that the maxillae opened and closed, while they remained stationary on the fronto-abdominal axis (without retraction).

5.4 | Labium

The only direction of movement for the labium during maximum angle measurements is the abducting to the posterior (Figure 15). With 71.5°, the measured mma was relatively large.

6 | DISCUSSION

6.1 | Labrum

A total of three different muscles were identified in the labrum, confirming the findings of Blanke et al. (2013). The muscle 0lb1 directly inserts into the labrum, while the muscle 0lb2 is connected to the anteclypeus. The muscles 0lb1 and 0lb2 are most likely used simultaneously to retract the labrum into the head cavity, a movement that is frequently observed in the feeding process, as also described by Popham and Bevans (1979). Accordingly, if only the muscle 0lb1 (or the muscle 0lb2, respectively) is contracted, it might lead to the tilting of the labrum to the frontal direction (Video S2), same as observed for dragonfly larvae (Büsse et al., 2021b). Muscle 0lb5 is a broad, dichotomous muscle connecting both frontal and abdominal inner walls of the labrum. We assume that this muscle

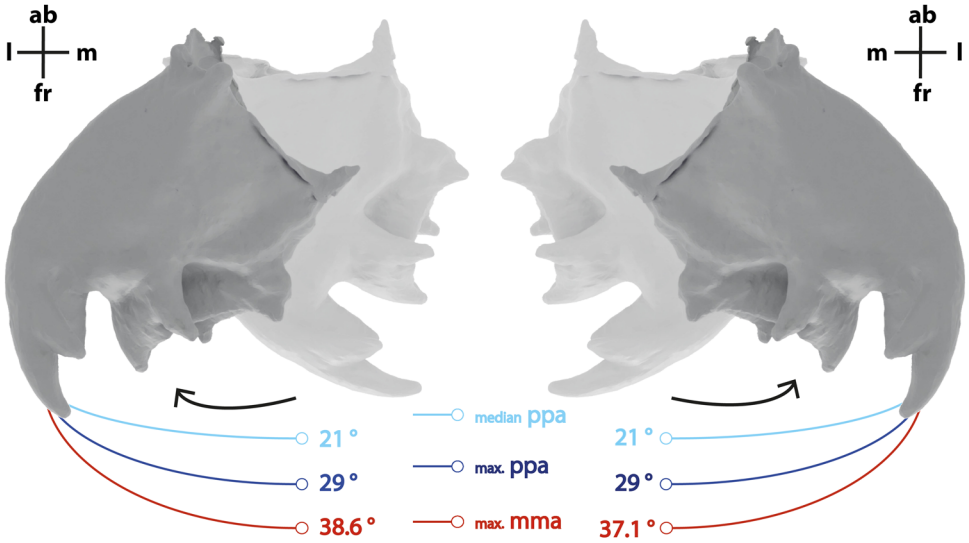

FIGURE 10 *Anax imperator*, visualization of the abduction movement of the mandibles, with maxmimum mma (red), maximum paa (dark blue) and median paa (light blue); anterior view. Although the paired mouthparts are most likely not identical in anatomy, the model of the right mandible was mirrored for the display of the left counterpart since the figures do not focus on anatomical information.

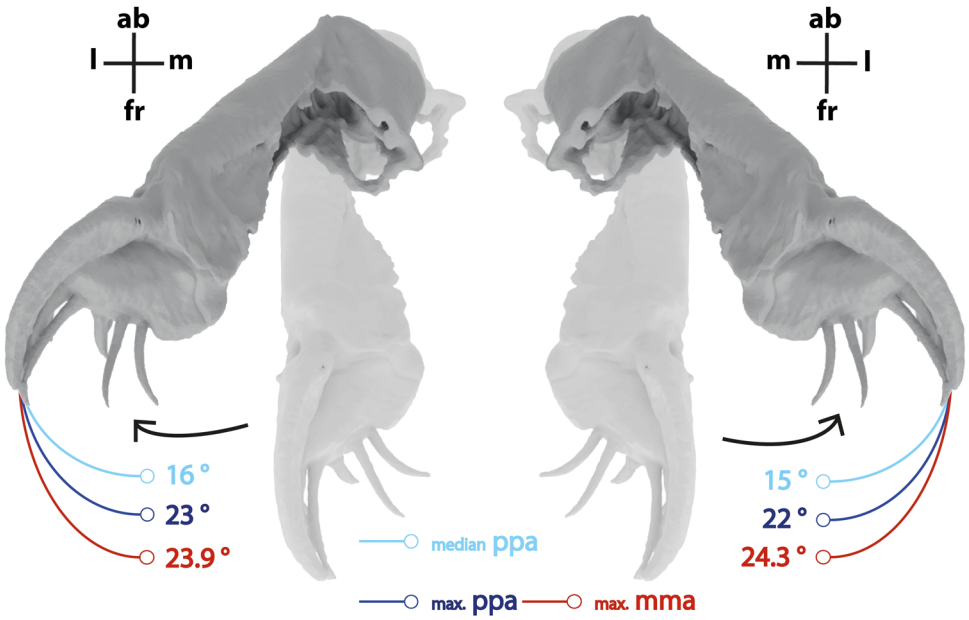

FIGURE 11 *Anax imperator*, visualization of the abduction movement of the maxillae (lateral direction), with maximum mma (red), maximum paa (dark blue) and median paa (light blue); anterior view. Although the paired mouthparts are most likely not identical in anatomy, the model of the right maxilla was mirrored for the display of the left counterpart since the figures do not focus on anatomical information.

functions to enlarge or flatten the labrum anterio-posteriorly, as also suggested to be the case in larvae (Büsse et al., 2017; Büsse et al., 2021b; Mathur & Mathur, 1961). However, this behavior is difficult to observe in recordings. On the abdominal surface of the labrum, the epipharnyx, numerous hair-like processes are found (Figure 5c,d). These are most likely chemo- (Haskell & Schoonhoven, 1969; Popham & Bevans, 1979) and mechanoreceptors (Rebora et al., 2014). Some of these receptors appear singularly on the epipharynx, while others are clustered together in groups. We assume the enlargement and flattening of the labrum, enabled by the muscle 0lb5, could enhance the contact formation of the labrum and the receptors with food items. Furthermore, this shape modulation might assist food handling, especially food intake.

There are multiple processes on the epipharynx of the labrum, which resemble large setae and smaller spines directed toward the mouth opening. These structures might hold crushed and sliced food until it can be moved to the oesophagus (Popham & Bevans, 1979; Richards & Richards, 1979). Although this specific behavior is difficult to observe in

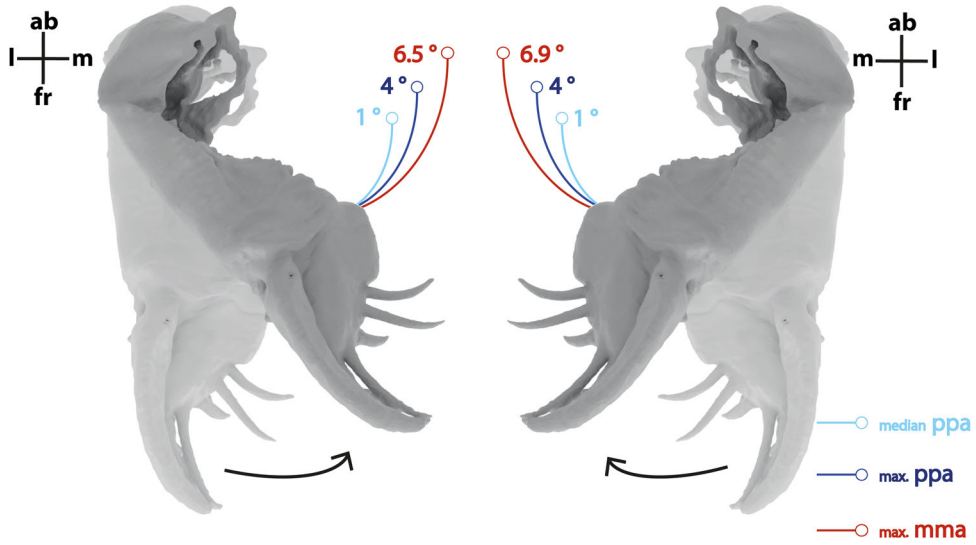

FIGURE 12 *Anax imperator*, visualization of the adduction movement of the maxillae (median direction), with maximum mma (red), maximum paa (dark blue) and median paa (light blue); anterior view. Although the paired mouthparts are most likely not identical in anatomy, the model of the right maxilla was mirrored for the display of the left counterpart since the figures do not focus on anatomical information.

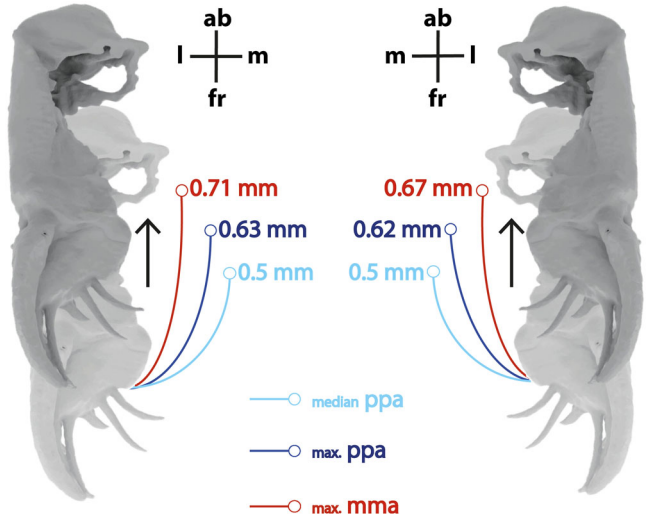

FIGURE 13 *Anax imperator*, visualization of the retraction movement of the maxillae (abdominal direction), with maximum mma (red), maximum paa (dark blue) and median paa (light blue); anterior view. Although the paired mouthparts are most likely not identical in anatomy, the model of the right maxilla was mirrored for the display of the left counterpart since the figures do not focus on anatomical information.

the videos, our results support the notion that the labrum plays an active role in the feeding process (Büsse et al., 2021b). Our recordings show frequent retraction and protraction of the labrum during feeding. Additionally, during mma measurements, we observed that the labrum can manually be retracted into the head until it is almost completely out of view. The labrum and more specifically the setae and spines on the epipharynx therefore could be utilized to scrape food particles towards the molar lobe of the mandibles for further processing. The enlargement of the labrum, controlled by the muscle 0lb5, might serve the purpose to tilt the epipharyngeal structures to reach more food items (Büsse et al., 2017).

The CLSM-results would, supposing the observed autofluorescence correlates with the material composition in a similar way as in other cuticle parts (e.g., Peisker et al., 2013), further support our hypothesis, since the large brushes of setae on the epipharynx (Figure 5b,c) seem to be partly sclerotized. This material composition could prove useful in moving food items towards the molar lobe. The setae might also be used as a cleaning tool, removing dirt and food particles from the mandibles during retraction. However, this hypothesis is difficult to confirm and such a behavior was not observed in the present study.

The material composition of the suture connecting the labrum to the anteclypeus seemingly consists of resilin-supplemented cuticle, which most likely facilitates the abducting movement of the labrum into the frontal direction as observed during the feeding process. The presence of resilin-matrices within this structure might enhance the flexibility and durability, as suggested by Büsse and Gorb (2018) for damselfly and by Büsse et al. (2021b) for dragonfly larvae. There are areas of the labrum which appear dark on the projection. This might be due to a certain degree of pigmentation, which inhibits autofluorescence. Without further methods like nanoindentation, no inferences towards the material composition of the parts of the cuticle which appear dark can be made at this point.

6.2 | Mandibles

The mandibles are used to dismember the prey, the incisor lobe piercing the outer shell/skin of the prey while the molar lobes further masticate the chunks of food; the latter grip together in a scissor-like

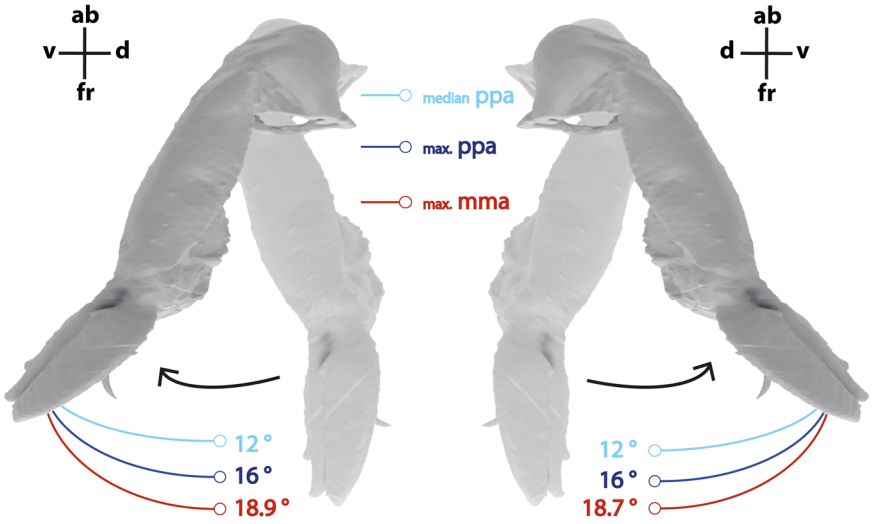

FIGURE 14 *Anax imperator*, visualization of the abduction movement of the maxillae (ventral direction), with maximum mma (red), maximum paa (dark blue) and median paa (light blue); lateral view. Although the paired mouthparts are most likely not identical in anatomy, the model of the right maxilla was mirrored for the display of the left counterpart since the figures do not focus on anatomical information.

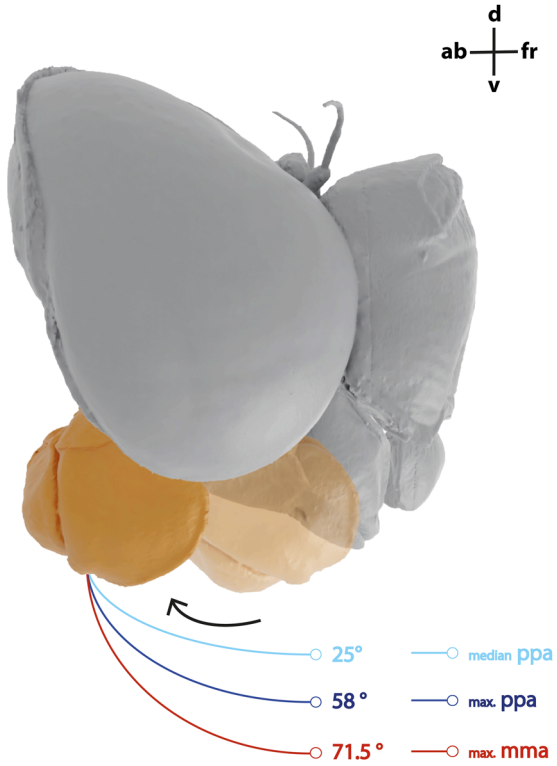

FIGURE 15 *Anax imperator*, visualization of the abduction movement of the labium (abdominal direction), with maximum mma (red), maximum paa (dark blue) and median paa (light blue); lateral view.

manner (Corbet, 2004; David et al., 2016). The ball-and-socket joints of the mandible allow only for a monoaxial movement, i.e., abduction and adduction (Asahina, 1954; Staniczek, 2000). We identified a total of six muscles in the mandible, the same as listed by Blanke et al. (2013). Muscle 0md1 is the adductor and muscle 0md3 the abductor of the mandible (Asahina, 1954; Büsse et al., 2017; Mathur & Mathur, 1961). The muscle 0md1 is by far the largest muscle in the head and can generate relatively high bite forces (David et al., 2016). The muscle 0md2 seems to be absent. Due to the appearance of the muscle 0md3 in dragonflies with its dichotomous attachment points, the muscle might be a fusion of both muscles 0md2 and 0md3 (Blanke et al., 2012). A total of four muscles (0md4–6, 0md8), which are rather inconspicuous, are attached to the inner wall of the mandible. According to the data of David et al. (2016) for *Sympetrum vulgatum* (Odonata: Anisoptera: Libellulidae), all these muscles, except 0md4, which was not explicitly mentioned, serve as additional adductor muscles. However, the amount of activation is relatively small and the contribution to the bite force performed by these muscles neglectable (David et al., 2016). Since the positioning and general geometry of the musculature in *A. imperator* is relatively similar, we assume that these muscles also serve as additional adductors. They might perform small modulating movements of the mandible to improve food mastication (Büsse et al., 2017, 2021b). The function of the muscle 0md4 is debatable, as it is rarely mentioned in the literature (Blanke et al., 2012). The muscle might support movement of the hypopharyngeal sclerites (cf. Büsse et al., 2017). The muscle 0md7 is absent, as assumed for all aeshnids (Short, 1954).

The mandibles are highly active during feeding. The variety of abduction distance most likely correlates with the size of the food item, although this would need further testing. Regarding the material composition, the large area of resilin-supplemented cuticle, which has been described as mandibular pad (Büsse & Gorb, 2018), is distinctive in the mandibles. However, it differs greatly from the one observed in damselfly (Büsse & Gorb, 2018) and dragonfly (Büsse et al., 2021b) larvae, regarding its shape and location. While in the larva of Odonata, the pad is more indistinctive and covers a larger area of the mandible, in adult *A. imperator* it is distinctive and clearly defined but limited to an area on the aboral part of the mandible (Figure 6). Since we measured a relatively large mma for the mandible, the pad might function as a damper to secure the mandible against collisions with the head capsule. Considering the large abduction distances observed, potential collisions with the head capsule are consequential. This function, relying on the flexibility of the cuticle, would be

congruent with observations made in different biomechanical systems of insects (Haas et al., 2000a; 2000b; Michels, Vogt & Gorb, 2012; Rajabi et al., 2016a, 2016b). Büsse and Gorb (2018) discussed the role of the mandibular pad in absorbing mechanical stress generated by the incisive teeth and the molar lobe, a function that could be attributed to the pad of *A. imperator* as well. Similar to the labrum, the mandibular cuticle shows areas with little to no autofluorescence. Again, this might be due to a certain pigmentation and, therefore, based on the CLSM-projections alone, no assumptions about the material composition can be made so far.

6.3 | Maxillae

The maxillae are used to grasp, perceive and handle food (Bassemir & Hansen, 1980; Pfau, 1986; Popham & Bevans, 1979). During the feeding process itself, they position the food item between the mandibles for processing (Büsse et al., 2021b; Popham & Bevans, 1979). In general, the movement of the maxillae is relatively unrestricted, as they are suspended to the head via membranous areas only (Asahina, 1954; Büsse & Gorb, 2018; Büsse et al., 2017). We identified a total of eight maxillary muscles, the same as presented by Blanke et al. (2013). The muscle 0mx1 is attached to the most dorsal part of the maxilla, the cardo, and most likely enables the retracting motion, as also suggested by Blanke et al. (2012) for *Epiophlebia superstes* and Büsse et al. (2017) for *Pyrrhosoma nymphula* larvae. The muscle 0mx2 is attached to the base of the lacinia and could function as a retractor as well, possibly facilitating a median movement of the distal end of the maxilla. The muscle 0mx3 is attached to the inner wall of the cardo, while both muscles 0mx4 and 0mx5 are attached to the stipes. The muscles 0mx3–5 might be used to perform the abducting movement of the maxilla, as well as the movements in ventral direction, due to the combination of different attachment point locations (Büsse et al., 2017, 2021b).

The muscle 0mx6 is attached to the base of the lacinia, which leads to our assumption that the lacinia might be movable independently of the stipes (cf. Büsse et al., 2017). In some recordings, we could indeed identify a movement that seems to be the lacinia alone, rather than the typical adducting motion of the entire maxilla (Büsse et al., 2021b; Popham & Bevans, 1979; Supporting Information Online Material, File S5). The material composition of the lacinia cuticle corroborates this hypothesis because the stipes-lacinia-suture is a syndesis (e.g., Neubert et al., 2017; Weihmann & Wipfler, 2019), which contains resilin-matrices, possibly supplemented by other proteins that promote flexibility, therefore facilitating movement. A similar function can be assessed at the maxillar palpus, it was observed that it can be flexed away from the lacinia to a great extent (Figure S7). The muscles 0mx8 and 0mx10 seem to be associated with the palpus and likely work opposed to each other as abductor and adductor. The fact that the palpus movement was observed in the videos complements the finding that the maxillary palpus of a damselfly is, much like the lacinia, connected to the maxilla via a syndesis (Büsse & Gorb, 2018). The fact that both the lacinia and the maxillar palpus can be moved independently could serve the purpose to further increase the capabilities of the maxillae to precisely handle food items, and especially of the maxillary palpus to sense the food via the associated chemoreceptors, similar to damselfly larvae (Bassemir & Hansen, 1980). Further looking into the lacinia, the dentisetae appear to be strongly sclerotized, however, they are connected to the lacinia by a resilin-supplemented base, the dentisetal pads. These pads most likely function as a dampening component for mechanical stress inflicted upon the dentisetae during feeding (Büsse & Gorb, 2018). Similar material compositions can also be found in the cardo of the maxilla, most notably the cardo-stipeal suture (Büsse & Gorb, 2018). The suture most likely works as a syndesis, enabling movement of the stipes, and implementation of resilin-matrices might be logical to enhance flexibility. In the present videos, aside from typical protraction and retraction, we could further identify an abducting motion in ventral direction as also found in a dragonfly larva (Büsse et al., 2021b). In the recordings, the retraction of both maxillae, as well as the abduction in ventral direction, seems to be synchronous, while the other movements are variable for both sides. The retracting motion is mostly noticed once the food item is grasped, therefore, a synchronous retraction of both maxillae is consequential, while the opening and closing movements serve to handle the food into a fitting position with desynchronized movements. The abduction in ventral direction seems to be rarely discussed in literature. From our observations (also cf. paa's), this capability of abduction is of importance during feeding since it adds another direction of movement. Without this mobility, the maxillae would simply move on a plane, comparable to the mandibles with additional retraction.

6.4 | Labium

The role of the labium within the feeding process is rather inconspicuous in adult *A. imperator*. It is suspended through an arthrodial membrane and seems to be limited to a monoaxial type of movement. We identified three labial muscles in the specimen, the same as presented by Blanke et al. (2013). The muscle system is reduced compared to that of the larvae (Büsse et al., 2017; Büsse et al., 2021a), a uniform tendency throughout odonates (Blanke et al., 2015; Short, 1954). The muscle 0la15 is most likely used as an abductor of the labium (Asahina, 1954; Mathur & Mathur, 1961). In larvae, due to the high mobility of the labium, it is also assumed that the muscle might prevent shearing of the labium against the head capsule (Büsse et al., 2017). The muscle 0la13 is attached to the base of the palpus and, therefore, might be used to control the labial palps. It is considerably larger and elongated in larvae and seems to enable movement of the palps together with the muscle 0la14 (Büsse et al., 2017); the latter is absent in adult *A. imperator*. The muscle 0la8 connects the prementum and the postmentum, possibly enabling a retracting motion of the distal labial part. In larvae, this muscle locks the movement of the joint in preparation of prey capture (Büsse et al., 2021a) of the highly modified raptorial labium—the so called

prehensile labial mask (Büsse et al., 2017; Büsse et al., 2021a; Corbet, 2004; Pritchard, 1965); no such function is present in the adults. The labial muscle 0la5, described in larvae as part of the independently loaded synchronized dual-catapult system, which drives the prehensile labial mask (Büsse et al., 2021a), is absent in adults. The hypopharyngeal muscle 0hy7, which connects to the labium, is present in both larval and adult dragonflies. In both cases, a retracting function is likely, although more pronounced in larvae (Büsse et al., 2017, 2021a). However, in the larvae muscle 0hy7 is another substantial muscle driving the mentioned catapult system (Büsse et al., 2021a). The large angles of movement for the opening motion are supplemented by the membranous suspension structures of the prementum. On the CLSM-projection, the prementum appears to consist mostly of membranous cuticle, maybe resilin-supplemented, which could explain the large angle it covers. It is unlikely that the animals are able to deflect the labium to large angles like 71.5° (the theoretical maximum) solely by using the muscles, as it is shown in the paa's (max. 55°). It is more likely that the food item pushes the labium open during feeding (Figure S8). The flexible composition of the premental cuticle could facilitate this movement, preventing damage.

The labium limits the oral cavity in abdominal and ventral directions, although it leaves the question whether it fulfills other functions during the feeding process. In this regard, the large end hooks on the labial palps (Asahina, 1954; Blanke et al., 2012) might be of interest. They are relatively well developed and sclerotized, but their mobility seems to be restricted to that of the palp itself. Although movements by the labial palps are observed during feeding, this movement is shallow, and it is difficult to estimate which purpose it serves. With that in mind, the end hooks might be used to enhance the grip of the mouthpart on the prey by puncturing it from the sides. However, the assumption mentioned above would need further investigation to reach a reliable conclusion. Additionally, several authors (Asahina, 1954; Blanke et al., 2012) described another distal structure on the labium as a movable hook. We were not able to identify a distinct movement from this structure, thus whether this movement is possible or not remains debatable. On the CLSM-projections, the movable hooks appear to be sclerotized, while the base of the hooks seems to be more flexible, possibly acting as a syndesis. This mixture of materials is comparable to the dentisetae and dentisetal pads and could therefore facilitate a similar function, i.e., solid cuticle to grab or puncture the food and a flexible base to prevent failure by mechanical stress.

6.5 | Biting and chewing

While examining the in vivo recordings, we observed two distinctively different types of concerted mouthpart movements, which are repeatedly used by the dragonflies during feeding. The first one we refer to as biting, as it involves the mandibles severing large parts out of the prey item, most notably using their incisive teeth (Video S2). During this process, the labrum often remains retracted and the labium is abducted, but inactive. The movement of the maxillae can be distinguished: i) open to grasp the food, or ii) remain closed posterior to the mandibles. The latter are highly active during biting, with large abduction distances to dismember the prey using the sclerotized incisive lobe. The biting behavior is contrasted by the chewing motion (Video S3). Here, the maxillae are more active, as they grasp and handle the prey. Subsequently, the maxillae pull the grasped food item towards the opened molar lobes of the mandibles for mastication and further processing. The paa´s of the mandibles during chewing are generally smaller compared to biting. During chewing, no single characteristic pattern of movement from the labrum and labium has been observed. They can be both protracted and retracted during two different chewing movements. The chewing motion we observed is comparable to the general feeding process described by Popham and Bevans (1979). Generally, the biting motion involves more activity by the mandibles, less by the maxillae. On the other hand, chewing displays more activity from the maxillae and only as much movement as necessary from the mandibles, probably depending on the food item size.

Similar observations have been described for *Periplaneta americana* (Blattodea: Blattidae; Schmitt et al., 2014): a cyclical, correlated movement of maxillae and mandibles during feeding. When the mandibles are abducted, the maxillae are simultaneously protracted and adducted. Since these movements are precisely coordinated, a strong neural correlation between movement of the mandibles and the maxillae is suggested, like a neural circuit specifically generating chewing patterns (Schmitt et al., 2014). Additionally, we observed and documented a behavior that did not seem to correlate directly with the feeding process. The dragonfly opens all mouthparts simultaneously to a large degree; a behavior that was observed three times in total over all recorded feeding processes (Video S4). The reason for this behavior remains unknown, as it occurred randomly with or without the presence of food. It could be a sort of aggressive defensive or threatening behavior, triggered by the circumstances of the experimental setup, although this would require further testing.

7 | CONCLUSIONS

We performed an analysis of the feeding process in the adult dragonfly *Anax imperator* using a multitude of methods, which enabled us to characterize the role of single mouthparts in the feeding process. We could show that the material composition of the cuticle most likely has a substantial effect on the functionality of the mouthparts. The presented methods complement each other and allow complex insights into a variety of aspects of the feeding process and its underlying biomechanics. Examples include the movement of the lacinia and the abducting motion of the labrum in frontal direction. Certain movements were analyzed morphologically by an estimation of mma's and further supplemented by the paa's. The underlying kinematics of these movements were

elucidated using the knowledge on the muscle attachment points (obtained from μCT) in combination with an analysis of the distribution of potentially flexible areas of the cuticle (obtained from CLSM-imaging of cuticular autofluorescence). The results offer comprehensive insights into the feeding kinematics for all mouthparts, including their theoretical maximum movement range. The presented set of methods needs to be further enhanced to form a base for comparative studies between insects with different lifestyles and feeding habits. Especially the measurement of true in vivo angles is of great interest to allow further insights, since here we were unable to present more than rough approximations (paa's).

NOMENCLATURE

Anatomical structures are described using the nomenclature of Beutel et al. (2014), muscle designations are made using the nomenclature of Wipfler et al. (2011). In the results, the muscles' points of insertion are abbreviated as 'I', points of origin as 'O'. The nomenclature of mouthpart structures related to the material composition follows Büsse and Gorb (2018).

AUTHOR CONTRIBUTIONS

Sebastian Büsse and Stanislav N. Gorb: designed the project and developed the concept of the study. **Benedikt Josten and Sebastian Büsse**: did the μCT and CLSM analysis and post-processing. **Benedikt Josten and Sebastian Büsse**: did the HS-video recordings. **Benedikt Josten**: did the angle measurements. All authors wrote the manuscript as well as read and approved the final version.

ACKNOWLEDGMENTS

We thank Esther Appel, Nienke Bijma, and Alexander Kovalev for their help. Furthermore, we thank Fabian Bäumler, Thies Büscher, Lena Hindenberg, Alexander Köhnsen and Dennis Petersen for discussions and/or proof-reading. This project and SB directly were financed by the DFG grant BU3169/1–2.

CONFLICTS OF INTEREST

The authors declare no conflicts of interests.

DATA AVAILABILITY STATEMENT

All data supporting our findings are presented in the paper and the supplementary material respectively. The raw data of the video footage can be found on Zendo: https://doi.org/10.5281/zenodo.6602654. The CT- and CLSM-raw data can be made available on reasonable request.

ORCID

Sebastian Büsse http://orcid.org/0000-0002-1657-7950

REFERENCES

Andersen, S. O. (1963). Characterization of a new type of cross-linkage in resilin, a rubber-like protein. *Biochimica et Biophysica Acta/General Subjects*, *69*, 249–262. https://doi.org/10.1016/0006-3002(63)91258-7

Andersen, S. O. (1964). The cross-links in resilin identified as dityrosine and trityrosine. *Biochimica et Biophysica Acta/General Subjects*, *93*, 213–215. https://doi.org/10.1016/0304-4165(64)90289-2

Andersen, S. O. (1979). Biochemistry of insect cuticle. *Ann Rev Entomol*, *24*, 29–61.

Asahina, S. (1954). A morphological study of a relic dragonfly *Epiophlebia superstes* Selys (Odonata, Anisozygoptera). *JSPS*, *1*, 1–153.

Bassemir, U., & Hansen, K. (1980). Single-pore sensilla of damselfly-larvae: Representatives of phylogenetically old contact chemoreceptors? *Cell and Tissue Research*, *207*, 307e320. https://doi.org/10.1007/BF00237814

Bäumler, F., & Büsse, S. (2019). Resilin in the flight apparatus of Odonata (Insecta)—cap tendons and their biomechanical importance for flight. *Biology Letters*, *15*(2019), 0127. https://doi.org/10.1098/rsbl.2019.0127

Beutel, R. G., Friedrich, F., Yang, X.-K., & Ge, S. Q. (2014). *Insect morphology and phylogeny: a textbook for students of entomology*. De Gruyter.

Blanke, A., Beckmann, F., & Misof, B. (2012). The head anatomy of *Epiophlebia superstes* (Odonata: Epiophlebiidae). *Org Divers Evol*, *13*, 55–66. https://doi.org/10.1007/s13127-012-0097-z

Blanke, A., Büsse, S., & Machida, R. (2015). Coding characters from different life stages for phylogenetic reconstruction: A case study on dragonfly adults and larvae, including a description of the larval head anatomy of *Epiophlebia superstes* (Odonata: Epiophlebiidae). *Zoological Journal of the Linnean Society*, *174*, 718–732. https://doi.org/10.1111/zoj.12258

Blanke, A., Greve, C., Mokso, R., Beckmann, F., & Misof, B. (2013). An updated phylogeny of Anisoptera including formal convergence analysis of morphological characters. *Syst Entomol*, *38*, 474–490. https://doi.org/10.1111/syen.12012

Burrows, M., & Sutton, G. P. (2012). Locusts use a composite of resilin and hard cuticle as an energy store for jumping and kicking. *Journal of Experimental Biology*, *215*, 3501–3512. https://doi.org/10.1242/jeb.071993

Büscher, T. H., Petersen, D. S., Bijma, N. N., Bäumler, F., Pirk, C. W. W., Büsse, S., Heepe, L., & Gorb, S. N. (2021). The exceptional attachment ability of the ectoparasitic bee louse *Braula coeca* (Diptera, Braulidae) on the honeybee. *Physiological Entomology*, *47*, 83–95. https://doi.org/10.1111/phen.12378

Büsse, S., Büscher, T. H., Heepe, L., & Gorb, S. N. (2019). Adaptations of dragonfly larvae and their exuviae (Insecta: Odonata), attachment devices and their crucial role during emergence. *Journal of Insect Physiology*, *117*, 103914. https://doi.org/10.1016/j.jinsphys.2019.103914

Büsse, S., & Gorb, S. N. (2018). Material composition of the mouthpart cuticle in a damselfly larva (Insecta: Odonata) and its biomechanical significance. *Royal Society Open Science*, *5*, 172117. https://doi.org/10.1098/rsos.172117

Büsse, S., Hörnschemeyer, T., & Gorb, S. N. (2017). The head morphology of *Pyrrhosoma nymphula* larvae (Odonata: Zygoptera) focusing on functional aspects of the mouthparts. *Frontiers in zoology*, *14*, 25. https://doi.org/10.1186/s12983-017-0209-x

Büsse, S., Koehnsen, A., Rajabi, H., & Gorb, S. N. (2021b). A controllable dual-catapult system inspired by the biomechanics of the dragonfly larvae's predatory strike. *Sci Robot*, *6*, eabc8170. https://doi.org/10.1126/scirobotics.abc8170

Büsse, S., Tröger, H.-L., & Gorb, S. N. (2021a). The toolkit of a hunter—Functional morphology of larval mouthparts in a dragonfly. *Journal of Zoology*, *315*, 247–260. https://doi.org/10.1111/jzo.12923

Corbet, P. S. (2004). *Dragonflies–Behaviour and ecology of Odonata. Revised edition*. Harley Books (B.H. and A. Harley Ltd).

Crampton, G. C. (1923). A phylogenetic comparison of the maxillæ throughout the orders of insects. *Journal of the New York Entomological Society*, *31*, 77–107.

David, S., Funken, J., Potthast, W., & Blanke, A. (2016). Musculoskeletal modelling of the dragonfly mandible system as an aid to understanding the role of single muscles in an evolutionary context. *Journal of Experimental Biology*, *219*, 1041–1049. https://doi.org/10.1242/jeb.132399

El-Gohary, M., & McNames, J. (2012). Shoulder and elbow joint angle tracking with inertial sensors. *IEEE Transactions on Biomedical Engineering*, *59*, 2635–2641. https://doi.org/10.1109/TBME.2012.2208750

Engel, M. S., Davis, S. R., & Prokop, J. (2013). *Insect wings: The evolutionary development of nature's first flyers. Arthropod biology and evolution: molecules, development, morphology* (pp. 269–298). Springer Verlag.

Frantsevich, L., Mokrushov, P., Shumakova, I., & Gorb, S. (1996). Insect rope-walkers: Kinematics of walking on thin rods in a bug, *Graphosoma italicum* (Heteroptera; Pentatomidae). *Journal of Zoology*, *238*, 713–724.

Gorb, S. N. (1995). Design of the predatory legs of water bugs (Hemiptera: Nepidae, Naucoridae, Notonectidae, Gerridae). *Journal of Morphology*, *223*, 289–302.

Gorb, S. N. (2004). The jumping mechanism of cicada *Cercopis vulnerata* (Auchenorrhyncha, Cercopidae): skeleton–muscle organisation, frictional surfaces, and inverse-kinematic model of leg movements. *Arthropod Struc Dev*, *33*, 201–220. https://doi.org/10.1016/j.asd.2004.05.008

Gröning, F., Jones, M. E. H., Curtis, N., Herrel, A., O'Higgins, P., Evans, S. E., & Fagan, M. J. (2013). The importance of accurate muscle modelling for biomechanical analyses: a case study with a lizard skull. *Journal of the Royal Society, Interface*, *10*, 20130216. https://doi.org/10.1098/rsif.2013.0216

Haas, F., Gorb, S. N., & Blickhan, R. (2000a). The function of resilin in beetle wings. *Proceedings of the Royal Society B: Biological Sciences*, *267*, 1375–1381. https://doi.org/10.1098/rspb.2000.1153

Haas, F., Gorb, S. N., & Wootton, R. J. (2000b). Elastic joints in dermapteran hind wings: Materials and wing folding. *Arthropod Struc Dev*, *29*, 137–146. https://doi.org/10.1016/s1467-8039(00)00025-6

Hao, Y. N., Sun, Y. X., & Liu, C. Z. (2020). Functional morphology of the mouthparts of lady beetle *Hippodamia variegate* (Coleoptera: Coccinellidae), with reference to their feeding mechanism. *Zoomorphology*, *139*, 199–212. https://doi.org/10.1002/jmor.20976

Haskell, P. T., & Schoonhoven, L. M. (1969). The function of certain mouthpart receptors in relation to feeding in *Schistocerca gregaria* and *Locusta migratoria* (Migratorioides).(migratorioides). *Entomologia Experimentalis et Applicata*, *12*, 423–440. https://doi.org/10.1111/j.1570-7458.1969.tb02538.x

Jandausch, K., Beutel, R., Pohl, H., Gorb, S. N., & Büsse, S. (2018). The legs of "spider associated" parasitic primary larvae of *Mantispa aphavexelte* (Mantispidae, Neuroptera)—Attachment devices and phylogenetic implications. *Arthropod Structure & Development*, *47*, 449–456. https://doi.org/10.1007/s00435-021-00524-6

Jansen, M. A., Niverty, S., Chawla, N., & Franz, N. M. (2021). Reducing the risk of rostral bending failure in *Curculio* Linnaeus, 1758. *Acta Biomaterialia*, *126*, 350–371. https://doi.org/10.1016//j.actbio.2021.03.029

Knoop, S., Vacek, S., & Dillmann, R. (2006). Sensor fusion for 3D human body tracking with an articulated 3D body model. *In Proc ICRA*, *57*, 1297–1298. https://doi.org/10.1016/j.robot.2008.10.017

Krenn, H. W. 2019. Form and function of insect mouthparts. Insect mouthparts: form, function, development and performance. Zoological Monographs, 5, Cham: Springer Nature, 9-64. https://doi.org/10.1007/978-3-030-29654-4_2.

Lerch, S., Zuber, R., Gehring, N., Wang, Y., Eckel, B., Klaas, K. D., Lehmann, F. O., & Moussian, B. (2020). Resilin matrix distribution, variability and function in *Drosophila*. *BMC Biology*, *18*, 195. https://doi.org/10.1186/s12915-020-00902-4

Li, C., Gorb, S. N., & Rajabi, H. (2021). Biomechanical strategies to reach a compromise between stiffness and flexibility in hind femora of desert locusts. *Acta Biomaterialia*, *134*, 490–498. https://doi.org/10.1016/j.actbio.2021.07.030

Losey, J. E., & Vaughan, M. (2006). The economic value of ecological services provided by insects. *BioScience*, *56*, 311–323. https://doi.org/10.1641/0006-3568(2006)56[311:TEVOES]2.0.CO;2

Mathis, A., Mamidanna, P., Cury, K. M., Abe, T., Murthy, V. N., Mathis, M. W., & Bethge, M. (2018). DeepLabCut: Markerless pose estimation of user-defined body parts with deep learning. *Nature Neuroscience*, *21*, 1281–1289. https://doi.org/10.1038/s41593-018-0209-y

Mathur, P. N., & Mathur, K. C. (1961). Studies on the cephalic musculature of adult *Ictinus angulosus* Selys (Odonata, Anisoptera, Gomphidae, Ictinae). *Journal of Morphology*, *109*, 237–249. https://doi.org/10.1002/jmor.1051090302

Matsuda, R. (1965). Morphology and evolution of the insect head. *Mem Am Inst Ent*, *4*, 1–334.

Mauss, V. (2007). Evolution verschiedener Lebensformtypen innerhalb basaler Teilgruppen der Faltenwespen (Hymenoptera, Vespidae). *Denisia 20, Kataloge der oberösterreichischen Landesmuseen Neue Serie*, *66*, 701–722.

Michels, J., & Gorb, S. N. (2012). Detailed three-dimensional visualization of resilin in the exoskeleton of arthropods using confocal laser scanning microscopy. *J Microsc*. *245*, 1–16. https://doi.org/10.1111/j.1365-2818.2011.03523.x

Michels, J., Vogt, J., & Gorb, S. N. (2012). Tools for crushing diatoms—opal teeth in copepods feature a rubber-like bearing composed of resilin. *Scientific Reports*, *2*, 465. https://doi.org/10.1038/srep00465

Moon, M. J., Park, J. G., & Kim, K. H. (2008). Fine structure of the mouthparts in the ambrosia beetle, *Platypus koryoensis* (Coleoptera: Curculionidae: Platypodinae). *Animal Cells and Systems*, *12*, 101–108. https://doi.org/10.1080/19768354.2008.9647162

Nath, T., Mathis, A., Chen, A. C., Patel, A., Bethge, M., & Mathis, M. W. (2019). Using DeepLabCut for 3D markerless pose estimation across species and behaviors. *Nature Protocols*, *14*, 2152–2176. https://doi.org/10.1038/s41596-019-0176-0

Neubert, D., Simon, S., Beutel, R. G., & Wipfler, B. (2017). The head of the earwig *Forficula auricularia* (Dermaptera) and its evolutionary implications. *Arthropod Syst Phylogeny*, *75*, 99–124.

Peisker, H., Michels, J., & Gorb, S. N. (2013). Evidence for a material gradient in the adhesive tarsal setae of the ladybird beetle *Coccinella septempunctata*. *Nature Communications*, *4*, 1661. https://doi.org/10.1038/ncomms2576

Petersen, D. S., Kreuter, N., Heepe, L., Büsse, S., Wellbrock, A. H. J., Witte, C., & Gorb, S. N. (2018). Holding tight to feathers—Structural specializations and attachment properties of the avian ectoparasite *Crataerina pallida* (Diptera, Hippoboscidae). *Journal of Experimental Biology*, *221*, 179242. https://doi.org/10.1242/jeb.179242

Pfau, H. K. (1986). Untersuchungen zur Konstruktion, Funktion und Evolution des Flugapparates der Libellen (Insecta, Odonata). *Tijdschrift voor Entomologie*, *129*, 35–123.

Popham, E. J., & Bevans, E. (1979). Functional morphology of the feeding apparatus in larval and adult *Aeshna juncea* (L.) (Anisoptera: Aeshnidae). *Odonatologica*, *4*, 301–318.

Pritchard, G. (1965). Prey capture by dragonfly larvae (Odonata; Anispotera). Canad. *Journal of Zoology*, *43*, 271–289.

Qian, Z. M., & Chen, Y. Q. (2017). Feature point based 3D tracking of multiple fish from multi-view images. *PLoS One*, *12*, e0180245. https://doi.org/10.1371/journal.pone.0180254

Rajabi, H., Shafiei, A., Darvizeh, A., Dirks, J.-H., & Gorb, S. N. (2016b). Effect of microstructure on the mechanical and damping behaviour of dragonfly wing veins. *Royal Society Open Science*, *3*, 160006. https://doi.org/10.1098/rsos.160006

Rajabi, H., Shafiei, A., Darvizeh, A., & Gorb, S. N. (2016a). Resilin microjoints: A smart design strategy to avoid failure in dragonfly wings. *Scientific Reports*, *6*, 39039. https://doi.org/10.1038/srep39039

Rebora, M., Gaino, E., & Piersanti, S. (2014). The epipharyngeal sensilla of the damselfly *Ischnura elegans* (Odonata, Coenagrionidae). *Micron*, *66*, 31–36.

Richards, A. G., & Richards, P. A. (1979). The cuticular protuberances of insects. *International Journal of Insect Morphology and Embryology*, *8*, 143–157. https://doi.org/10.1016/0020-7322(79)90013-8

Rüppell, G., & Hilfert, D. (1993). The flight of the relict dragonfly Epiophlebia superstes (Selys) in comparison with that of the modern Odonata (Anisozygoptera: Epiophelebiidae). Odonatologica. 22, 295–309.

Schmitt, C., Rack, A., & Betz, O. (2014). Analyses of the mouthpart kinematics in *Periplaneta americana* (Blattodea, Blattidae) by using synchrotron-based X-ray cineradiography. *Journal of Experimental Biology*, *217*, 3095–3107. https://doi.org/10.1242/jeb.092742

Scudder, G. G. E. (2009). The importance of insects. *Insect biodiversity*, *Wiley-Blackwell*, *Chichester*, *1*, 7–32.

Short, J. R. T. (1954). The morphology of the head of *Aeshna cyanea* (Müller) (Odonata: Anisoptera). *Ecological Entomology*, *106*, 197–211.

Snodgrass, R. E. (1935). *Principles of insect morphology*. McGraw-Hill Book.

Staniczek, A. H. (2000). The mandible of silverfish (Insecta: Zygentoma) and mayflies (Ephemeroptera): Its morphology and phylogenetic significance. *Zoologischer Anzeiger*, *239*, 147–178.

Theriault, D. H., Wu, Z., Hristov, N. I., Swartz, S. M., Breuer, K. S., Kunz, T. H., & Betke, M. (2010). Reconstruction and analysis of 3D trajectories of Brazilian free-tailed bats in flight. computer science technique report BUCS-TR-2010-027. *Boston Univeristy*, *Boston*, *Mass*, *39*, 1–7. https://doi.org/10.5589/m13-034

Tillyard, R. J. (1917). *The biology of dragonflies (Odonata or Paraneuroptera)* (pp. 9–19). Cambridge University Press

Vincent, J. F. V., & Wegst, U. G. K. (2004). Design and mechanical properties of insect cuticle. *Arthropod structure & development*, *33*, 187–199. https://doi.org/10.1016/j.asd.2004.05.006

Weihmann, T., Reinhardt, L., Weißing, K., Siebert, T., & Wipfler, B. (2015). Fast and powerful: Biomechanics and bite forces of the mandibles in the American cockroach *Periplaneta americana*. *PLoS One*, *10*, e0141226. https://doi.org/10.1371/journal.pone.0141226

Weihmann, T., & Wipfler, B. (2019). The generalized feeding apparatus of cockroaches: A model for biting and chewing insects. *Insect Mouthparts: Form, Function, Development And Performance*, *5*, 203–262. https://doi.org/10.1007/978-3-030-29654-4_7

Weis-Fogh, T. (1960). A rubber-like protein in insect cuticle. *Journal of Experimental Biology*, *37*, 889–907.

Weis-Fogh, T. (1961). Molecular interpretation of the elasticity of resilin, a rubber-like protein. *Journal of Molecular Biology*, *3*, 648–67.

Weisser, W. W., & Siemann, E. (2008). *The various effects of insects on ecosystem functioning. Ecological studies (analysis and synthesis)*. Springer. https://doi.org/10.1007/978-3-540-74004-9_1

Wipfler, B., Machida, R., Müller, B., & Beutel, R. G. (2011). On the head morphology of Grylloblattodea (Insecta) and the systematic position of the order, with a new nomenclature for the head muscles of Dicondylia. *Syst Entomol*, *36*, 241–266. https://doi.org/10.1111/j.1365-3113.2010.00556.x

Zhang, W., Li, M. H., Zheng, G. B., Guan, Z. J., Wu, J. N., & Wu, Z. G. (2019). Multifunctional mandibles of ants: Variation in gripping behavior facilitated by specific microstructures and kinematics. *Journal of Insect Physiology*, *120*, 103993. https://doi.org/10.1007/s42235-020-0065-9

SUPPORTING INFORMATION

Additional supporting information can be found online in the Supporting Information section at the end of this article.

How to cite this article: Josten, B., Gorb, S. N., & Büsse, S. (2022). The mouthparts of the adult dragonfly Anax imperator (Insecta: Odonata), functional morphology and feeding kinematics. *Journal of Morphology*, 283(9), 1163–1181. https://doi.org/10.1002/jmor.21497